Journal of Water Resource and Protection, 2022, 14, 680-697
https://www.scirp.org/journal/jwarp
ISSN Online: 1945-3108
ISSN Print: 1945-3094

An Overview of the Geological Control on Groundwater Potential in Lacamutu River, Alaua Kraik Area, Baucau Municipality, Timor-Leste

Mafaldo Jose Faria, Marcal Ximenes, Jonas Sambi da C. Amaral, Amandio da Silva

Instituto do Petróleo e Geologia—Instituto Publico (IPG-IP) Division of Hydrogeology & Mineral Resources, Hydrogeology Team, Dili, Timor-Leste
Email: mfaria@ipg.tl

How to cite this paper: Faria, M.J., Ximenes, M., Amaral, J.S.D.C. and da Silva, A. (2022) An Overview of the Geological Control on Groundwater Potential in Lacamutu River, Alaua Kraik Area, Baucau Municipality, Timor-Leste. *Journal of Water Resource and Protection*, **14**, 680-697.
https://doi.org/10.4236/jwarp.2022.1410036

Received: June 15, 2022
Accepted: October 14, 2022
Published: October 17, 2022

Abstract

Timor island has a tropical climate with relatively little rainfall and surface water is often not available throughout the year with groundwater relied on to fulfill daily domestic necessities. Geological reconnaissance mapping, hydrogeological investigation, and resistivity survey were undertaken in this study to systematically understand the hydrogeologic system (e.g., aquifer system, hydrostratigraphic units, groundwater flow direction) and its potentiality for water supply to human consumption in Alaua Kraik area, Baucau Municipality, Timor-Leste. Res2DInv, Dips 5.1, Surfer 16, Global Mapper 13, and ArcGIS 10.6 software was used to create geological reconnaissance maps, resistivity interpretation profile lines, and a hydrostratigraphic model. Rainfall precipitation, rainfall intensity, maximum rate of runoff and infiltration data are also used to interpret the groundwater potential in the study area. Two rock units occur in the study area; permeable alluvial deposits which unconformable overlie impermeable interbedded red marl-chert and calcareous shale. Structurally the area comprises the Lacamutu anticline, thrust fault, left slip fault, and normal right slip fault. Resistivity lines indicate three (3) types of lithologies: alluvial deposit, an intercalated layer of red marl-chert, calcareous shale and wet calcareous shale. The alluvial deposit and red marl-chert layer intercalated with calcareous shale units are classified as a hydrostratigraphic unit of intergranular and localised aquifer systems with low productivity. The groundwater flows through the existing fractures of the shear joint and tends to flow towards the left slip fault plane zone from the North to South direction. Much of the rainwater in the study area is most likely intercepted, evaporated, and or transpiration as opposed to running off and infiltrating into the ground. The permeable and heavily fractured impermeable rock units in the study area have good porosity but low permeability and represent poor aquifers. The springs and Lacamutu River have low discharge and are generally dry in the dry season as it does not have an adequate aquifer that can accumulate and pass groundwater with significant volumes even if the rainfall in the study area is classified as moderate rainfall.

Keywords

Local Geology, Resistivity Interpretation, Groundwater Potential, Rainfall, Lacamutu River—Alaua Kraik Area—Timor-Leste

1. Introduction

Groundwater is among the most valuable natural resources supporting human health, economic development, and ecological diversity [1] [2]. The importance of groundwater is growing in both urban and rural areas of many countries [3] due to the increasing demand and pressure from population growth, irrigated agricultural activities and climate change [4] [5]. Most of Timor island has a tropical climate but with small rainfall compared to the other tropical countries due to its geographical location near the equator [6]. As a result, surface water is not obtainable throughout the year and groundwater is required to meet daily domestic industrial and agricultural [7] [8] [9] [10] [11]. Groundwater occurrence, source and movement are dependent on the geological characteristics such as rock type, thickness, structures, and permeability of aquifers [1]. Hence, geological reconnaissance mapping, hydrogeological investigations, and resistivity surveys are applied in this study to systematically assess groundwater conditions and their potential to supply water for human consumption. The domestic water supply for the local community in the study area is still depending on dug wells, springs, and main rivers. However, these are limited in both quantity and quality and cannot fulfill the demand for clean water, especially during the long dry season [12].

The 0.95 km^2 study area is located in Alaua Kraik village near the Lacamutu River in Baguia Administrative Post (Baucau Municipality) ~150 km from the Capital City of Dili (**Figure 1**). It is low terrain topography with a contoured index ranging from 110 - 240 m.

The chaotic geology of Timor island is part of the non-volcanic Outer Banda Arc formed through the collision between Sundaland (Southeast Eurasia) and the Australian continent in the late Neogene [13]-[18]. The regional lithologic formation within the study area are Pre-Permian low-grade to moderate metamorphic rocks associated with ultrabasic gabbro to dolerite rock units of the Lolotoe Complex; a Cretaceous chert interbedded with calcareous shale of Borolalo Limestone; Holocene unconsolidated sediment of Alluvial deposits; Permian biocalcarenite and crinoid limestone of the Maubisse Formation; and Upper

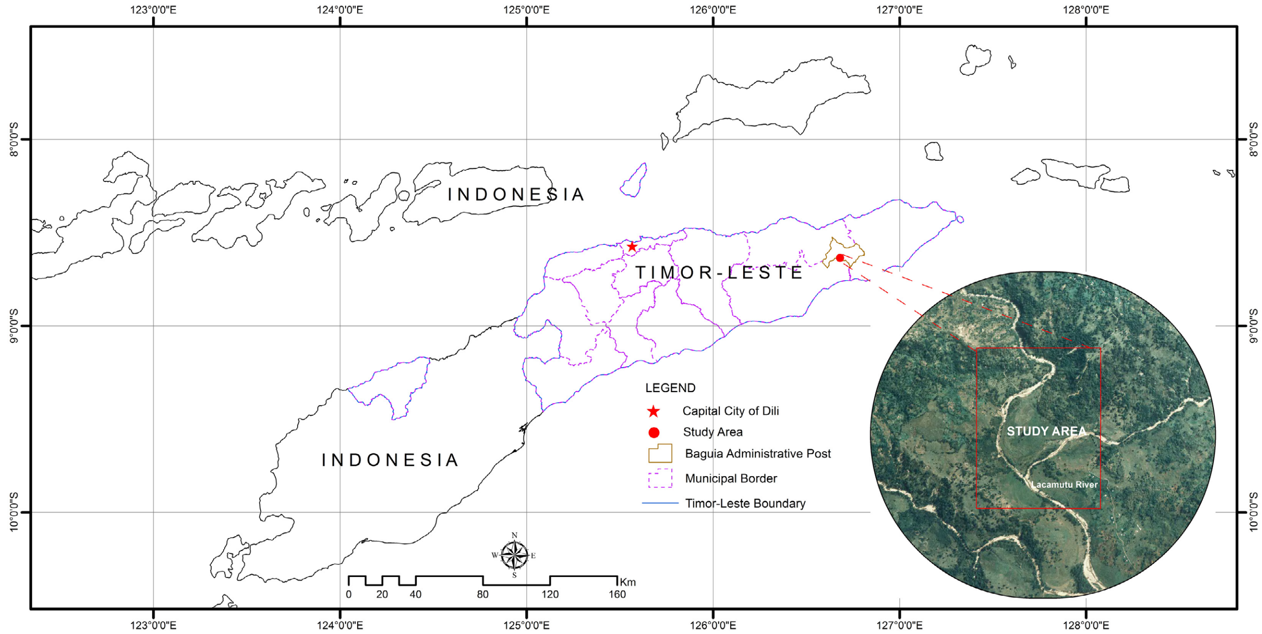

Figure 1. The study area of Lacamutu River, Alaua Kraik, Baguia Administrative Post, Baucau Municipality, Timor-Leste.

Miocene chaotic rocks of boulder-sized fragments within scaly clay matrix of Bobonaro Scaly Clay [19] [20]. All these lithologic units are classified as impermeable and are not likely to work as aquifers based on their thickness, porosity, and permeability.

In August 2021, only 65% (265) out of 408 households in Alaua Kraik area had been access to clean water, while 35% (143) reminds unobtainable [12]. In addition, surface water distribution including river and watersheds in the study area are mainly derived from rainfall and springs and are all categorized as intermittent types. Therefore, most of the local population lack clean water supply for their daily domestic needs during the long dry season [12]. To understand potential ways of mitigating this, the objectives of the study were as follows: 1) identify the available groundwater resources in the study area and estimate its potential for human consumption, 2) to define the aquifer system, the hydrostratigraphic units, and the groundwater flow direction modeling concept via geological reconnaissance mapping, resistivity study and well-log data.

2. Literature Review

The main origin of groundwater is rainwater. Rainwater that falls on the surface will flow as runoff and some will infiltrate into the ground through the infiltration process [21]. Infiltration is the flow of water (rain) into the soil as a result of capillary forces and gravity. After the topsoil layer is saturated, the water surplus flows into the deeper ground because of the earth's gravity, commonly called percolation [22]. The amount of water that flows downward depends on the type of soil or rock itself [23], while the capacity to infiltrate rainwater is expressed as the infiltration capacity, which is mostly affected by several factors including soil surface conditions, soil structure, vegetation, soil temperature, etc. Infiltration capacity can be approached by knowing the porosity of a rock or soil (**Table 1**).

Groundwater is naturally limited by hydraulic boundaries which are effectively controlled by the geological and hydrogeological conditions of the local area [24]. The important factor that influences the process of groundwater formation is geological rock units, which are lithologic formations or other geological materials that store large amounts of groundwater, naturally known as aquifers [25].

The ability of a rock to store and pass water is largely specified by the porosity and permeability of the rock itself. Porosity defines the amount of water that can be accumulated in geological substrate whereas permeability describes how those pores are interconnected and determines water flow from one pore to the next [26]. The porosity and permeability help to define the hydrogeologic characteristics of rock units. The presence of fractures (secondary porosity) and the thickness of the material overlying the rock are factors that control groundwater storability and potential [21] [27] [28]. The type of porosity varies greatly depending on its genesis, cavity size, and the relation between pores which are affected by compaction, cementation, grain size, grain form, grain structure, and grain sorting, and it can be classified as large porosity, if it is greater than 20%, medium porosity ranges from 5% to 20%, and small porosity if it has a value of less than 5% (**Table 2**). High porosity is not a definitive indication that an aquifer will produce a large volume of water for a well. Meanwhile, factors that affect permeability are grain size, grain form, sorting, degree of compactness, and cementation thereof it appears the different values of permeability for several rock types [21] (**Table 3**).

Table 1. The infiltration texture ranges based on the rock porosity [21].

No.	Material	Porosity (%)	No.	Material	Porosity (%)
1	Coarse gravel	28	**13**	Coarse sandstone	45
2	Medium gravel	32	**14**	Loose material	49
3	Gravel	34	**15**	Peat	92
4	Coarse sand	39	**16**	Schist	38
5	Medium sand	39	**17**	Mudstone	35
6	Fine sand	43	**18**	Claystone	43
7	Mud (silt)	46	**19**	Shale	6
8	Clay	42	**20**	Tuff	41
9	Fine grain sandstone	33	**21**	Basalt	17
10	Medium sandstone	37	**22**	Weathered gabro	43
11	Limestone	30	**23**	Weathered granite	45
12	Dolomite	26			

Table 2. The magnitude of rock porosity [21].

No.	Material	Porosity (%)	No.	Material	Porosity (%)
1	Soil	50 - 60	**7**	Gravel	30 - 40
2	Clay	45 - 55	**8**	Gravel and sand	20 - 35
3	Mud (silt)	40 - 50	**9**	Sandstone	10 - 20
4	Medium sand and coarse	35 - 40	**10**	Shale	1 - 10
5	Uniform sand	30 - 40	**11**	Limestone	1 - 10
6	Fine sand and medium	30 - 35			

Table 3. The permeability in several types of rocks [21].

Permeability	High				Medium					Low			
Sand & Gravel (not combined)	Separated gravel			Separated sand, sand & gravel			Fine grain sand, mud (sill) & clay						
Combined Rock	Rock with most fractured				Oil reservoir rock			Sandstone		Limestone, Dolomite		Granite	
k (cm^2)	10^{-3}	10^{-4}	10^{-5}	10^{-6}	10^{-7}	10^{-8}	10^{-9}	10^{-10}	10^{-11}	10^{-12}	10^{-13}	10^{-14}	10^{-15}
k (millidarcy)	10^{8}	10^{7}	10^{6}	10^{5}	10^{4}	10^{3}	100	10	1	0.1	0.01	10^{-3}	10^{-4}

Naturally, rock units that act as a medium for groundwater flow have favorable permeability, specific capacity, transmissivity, and storage where only lithologic permeability is able to consider in this study. According to Darcy [21], there is a relationship between permeability (k), laboratory coefficient of permeability (Ks), rock types, and their characteristics to groundwater flow (**Table 4**).

The existence of groundwater is very specific, and its distribution is also uneven depending on the geological subsurface conditions such as the distribution of permeable and impermeable layers. Accordingly, in determining the presence of groundwater it is necessary to do a geological subsurface study through resistivity surveys. The various resistivity values of rock units rely on the lithologic parameters themselves. These parameters are porosity and fluid contents (oil, gas, and groundwater). Typically, igneous and metamorphic rocks have high resistivity values. The resistivity of these rocks depends on their structure, texture, and the percentage of fractures that have been filled by groundwater [29]. The high porosity of sedimentary rocks which have been filled up by the fluids has lower resistivity than the consolidated sedimentary rocks with resistivity values less than 1000 Ω·m whereas the unconsolidated material of sedimentary has lower resistivity values than sedimentary rocks. Groundwater has numerous resistivity relying on the concentration of salt dissolution with resistivity values ranging from 10 - 100 Ω·m. The resistivity values that are less than <0.2 Ω·m are usually found in seawater due to a high salt composition (**Figure 2**). Furthermore, the resistivity of each material in the earth has a typical interval range, **Table 5** below displays the variation of the resistivity values of rock materials, minerals, and various fluids.

Table 4. The relationship between k, Ks, rock types, and their properties towards groundwater flow [21].

	Specific permebility, k, darcys										
	10^5	10^4	10^3	10^2	10	1	10^{-1}	10^{-2}	10^{-3}	10^{-4}	10^{-5}
Soil class		Clean gravels			Clean sands; mixtures of clean sands and gravels			Very fine sands; silts; mixtures of sand, silt, and clay; stratified clays; etc.		Unweathered clays	
Flow characteristics				Good aquifers				Poor aquifers		Impervious	
		10^6	10^5	10^4	10^3	10^2	10	1	10^{-1} / 10^{-2}	10^{-3}	10^{-4}
	Laboratory coefficient of permeability, Ks, gal/day/ft^2										

Table 5. The resistivity value of rocks, minerals, and various fluids [29] [31] [32] [33].

Type of Material	Resistivity Value (Ω·m)	Type of Material	Resistivity Value (Ω·m)
IGNEOUS ROCK			
Diorite	10^4 - 10^5	Peridotite	3×10^3 (wet) - 6.5×10^3 (dry)
Basalt	10 - 10^7 or 10^3 - 10^6	Andesite	4.5×10^4 (wet) - 1.7×10^2 (dry)
Lava	300 - 10,000	Tuff	2×10^3 (wet) - 10^5 (dry)
Granite	3×10^2 - 10^6 or 10^2 - 10^6	Gabbro	10^3 - 10^6
METAMORPIC ROCK			
Slate	3×10^2 - 4×10^7	Gneiss	6.8×10^4 (wet) - 3×10^6 (dry)
Marble	10^2 - 2.5×10^8	Schist	10 - 10^4
Hornfels	8×10^3 (wet) - 6×10^7 (dry)	Quartzite	10 - 2×10^8
Graphite Schist	10 - 10^2	Slate Group	200 - 2000
SEDIMENTARY ROCK			
Alluvium & sand	10 - 800 or 4 - 800	Marl	20 - 200 or 8 - 100 or 3 - 70
Dolomite	10^2 - 10^4 or 3.5×10^2 - 5×10^3	Claystone	10 - 10^8 or 8 - 100
Sand	1 - 100 or 100 - 600	Clay	1 - 100 or 2 - 20 or 3 - 30
Argillites	10 - 8×10^2	Conglomerates	2×10^3 - 10^4 or 100 - 500
Shale	300 - 3000 or 8 - 100	Alluvium	10 - 800
Limestone	50 - 10^7 or 50 - 400 or 300 - 10,000	Gravel	100 - 600
Mudstone	20 - 200	Sand and gravel	100 - 1000 or 1000 - 10,000
Chert group	200 - 2000	Argillaceous sand	5 - 50
MINERAL			
Copper (Cu)	1.7×10^{-8}	Gold (Au)	2.4×10^{-8}
Silver (Ag)	1.6×10^{-8}	Graphite (C)	10^{-3}
Iron (Fe)	10^{-7}	Manganese (Mn)	48.2×10^{-8}
Hematite (Fe_2O_3)	10^{-2} - 10^6	Calcite ($CaCO_3$)	5.5×10^{13}

Continued

Quartz (SiO_2)	4×10^{10}	Aluminum (Al)	2.65×10^{-8}
Bauxite ($Al_2H_2O_4$)	2×10^2 - 6×10^{-3}	Pyrite (FeS_2)	3×10^{-1}
Galena (PbS)	2×10^{-3}	Sphalerite (ZnS)	100
SOIL & FLUID			
Moist bedrock	150 - 300	Top soil	50 - 100
Sandy silt soil	15 - 150	Brackish water	0.3 - 1
Sea water	0.2	Salt water	0.05 - 0.2 or 0.5 - 5 or 0.5 - 1
Sand and gravel containing salt water	0.5 - 5	Sand and gravel containing fresh water	50 - 500
Soil	1 - 10	Surface water	80 - 200 or 30 - 3×10^3
Groundwater	30 - 100 or 40 - 6×10^2 or 10 - 100	Clay and soil	1 - 10,000
Fresh water	5 - 100	Oil sand	4 - 800

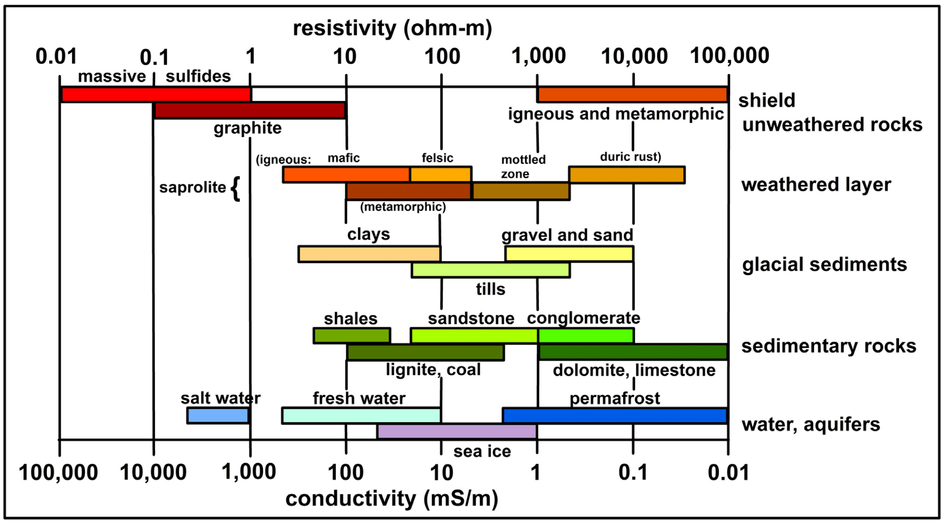

Figure 2. The electrical resistivity and conductivity values for selected materials [30].

3. Methodology and Materials

The study applies two (2) main methodological approaches, including geological reconnaissance mapping and resistivity surveys to identify the groundwater resources in the study area. The geological reconnaissance mapping method was applied thru field observations of geological structures and lineament interpretation from DEM (*Digital Elevation Model*), observations of rock units, descriptions of rock samples from well-log, and also identification of springs in the Lacamutu River area of Alaua Kraik. The resistivity study method is a geoelectric survey to detect subsurface lithologic conditions in a certain depth that will appear to indicate the hydrostratigraphic units of the subsurface and the presence of groundwater.

Geological structure data were analyzed using Dips 5.1 stereograph software to identify and characterize the structures. The rock units were described petrographically by using a polarized microscope to determine the types and the characteristics of the rock units themselves. Springs mapping was undertaken together with the measurement of discharge through volumetric measurement method. The 2-D resistivity survey used the *Resistivity Meter McOHM Profiler 4* Instrument of Pole-Pole configuration with current electrodes spread (AB) of 160 m that can reach a maximum depth of 130 m. The rainfall precipitation data in the Baguia Administrative Post, from the [34] rainfall station during the period time of 2010 to 2018 was also calculated to determine the rainfall intensity, maximum rate of runoff [35], and infiltration [22] [23] based on the following equation:

$$I = R_{24}/24\left(24/t\right)^{2/3}$$

where:

I = rainfall intensity (mm/hour);

t = duration of rain (hour);

R_{24} = the maximum rainfall for 24 hours (mm).

$$Q = c/360\left(I \times A\right)$$

where:

Q = maximum rate of runoff (m^3/s);

I = rainfall intensity (mm/hour);

A = catchment area (Km^2);

c = values of the runoff coefficient [36].

$$I = k \times Q$$

where:

I = infiltration (mm/s),

k = infiltration capacity (%);

Q = maximum rate of runoff (m^3/s).

All geological observation data were integrated into a shapefile and then displayed in ArcGIS 10.6 along with the other related data to create a data-based geological reconnaissance map. The resistivity data were analyzed and interpreted using Res2DInv Software and Golden Software's Surfer 16, numbers in **Figure 2** and **Table 5**, and the geological reconnaissance map. The geological cross-section lines are used to define the hydrogeological units for groundwater potential in the study area. Resistivity profile lines and well-log data were utilized to interpret the thickness of lithologic layers of subsurface, groundwater distribution, and the hydrostratigraphic units of the subsurface. Moreover, the aquifer system, the hydrostratigraphic units, and the groundwater flow direction concept are illustrated and modeled based on the geological reconnaissance map, resistivity interpretation, and well-log data in Global Mapper 13 and ArcGIS 10.6. Lastly, the data on rainfall precipitation, rainfall intensity, maximum rate of runoff, and infiltration are also used to constrain the groundwater potential in the study area.

4. Result and Discussion

Geology of the Study Area

Observation in the study area indicates the presence of both unconsolidated permeable and consolidated impermeable rock units. The fluvial deposits of the unconsolidated permeable sediment comprise various types of rock fragments including carbonate breccia chert, calcareous shale, breccia pumice, calcareous massive, chert with calcite intercalation, green shale, igneous mafic, crinoid limestone, red marl, and calcarenite. In the outcrop, the well-exposed light gray of fluvial deposits display normal bedding structure with poorly sorted grains ranging from angular boulder to clay size with a mud-clay matrix and opened fabrics along the river terraces where it was deposited with strong energy. The consolidated impermeable rock units are also displaying normal bedding structure and comprise interbedded red marl-chert and calcareous shale. The fluvial deposit has a thickness of about 3 meters and lies unconformably on the underlying consolidated impermeable units moreover, petrographic analysis of the sedimentary rocks intercalation hint at two (2) rock units, *i.e.*, calcareous shale and marl (**Figure 3**). Well logs show that unconsolidated fluvial deposits are present

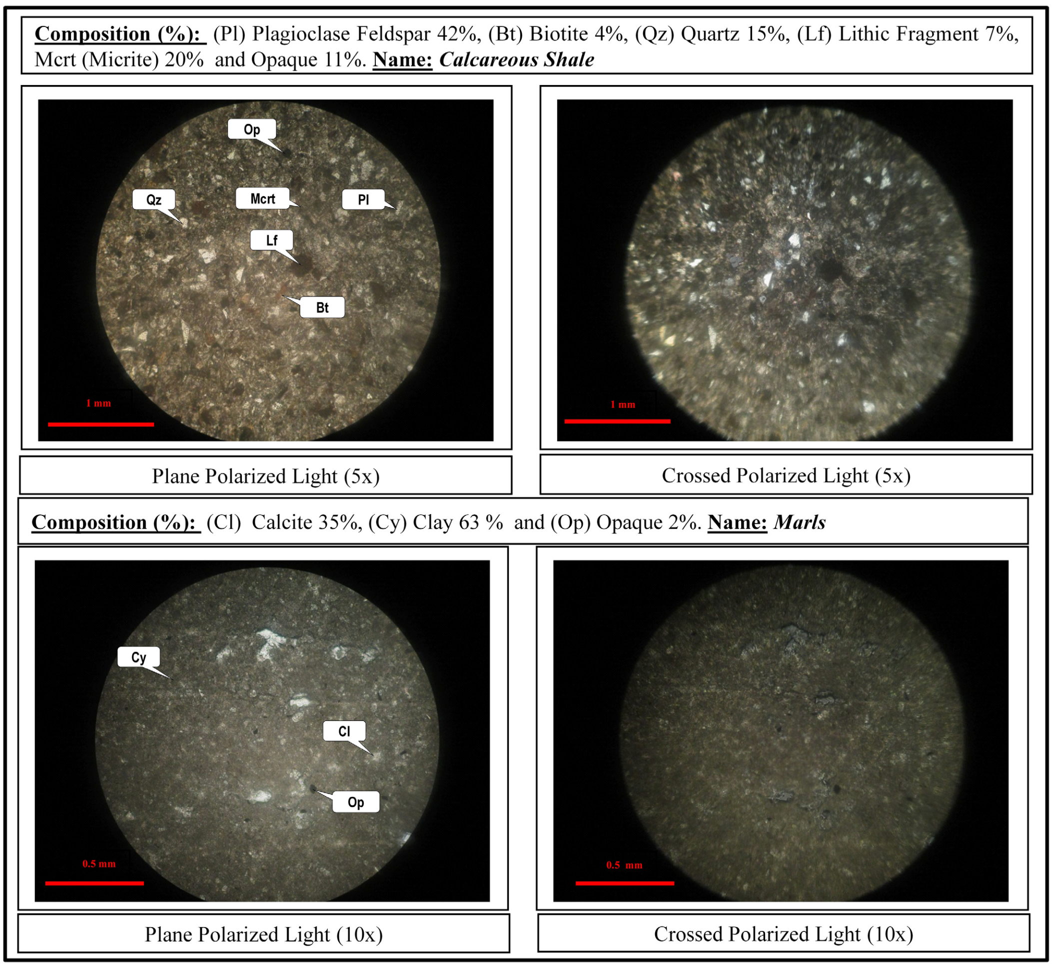

Figure 3. The petrographic analysis of consolidated impermeable materials of calcareous shale and marl.

from 0 to 3 m depth; from 3 to 5 m is an impermeable layer of calcareous shale; from 5 to 18 m are impermeable red marl-chert; from 18 to 19 m is calcareous shale, and from 19 to 25 m there is red marl- chert.

DEM (*digital elevation model*) interpretation shows a general ridge and valley direction of Northeast-Southwest (N 334˚ E) with principal stress of $\sigma 1$ = N 10˚ E, $\sigma 2$ = N 0˚ E and $\sigma 3$ = N 276˚ E (**Figure 4**).

Field mapping in the study area indicates there are four (4) types of geological structures present; **1)** *normal right slip fault* [37], indicated by gash fractures found in the calcareous shale unit with fault plane of N 152˚ E/88˚, direction N 262˚ E/78˚ and stress direction $\sigma 1$ = 4˚, N 81˚ E, $\sigma 2$ = 79˚, N 330˚ E, $\sigma 3$ = 10˚, N 170˚ E, rake 12, Net Slip 81˚, N 326˚ E. The structure of *normal right slip fault* has been formed by *left slip fault* with the direction of N 5˚ E/78˚; **2)** *left slip fault*, observed in the impermeable red marl-chert and calcareous shale unit with direction of N 5˚E/78˚ which crosses over the *thrust fault* with West-East direction; **3)** *anticline upright horizontal fold* [38] by Northwest-Southeast direction, direction limb 1= N 315˚ E/35˚, limb 2 = N 144˚ E/32˚, stress direction $\sigma 1$ = 4˚, N 229˚ E, $\sigma 2$ = 4˚, N 319˚ E, $\sigma 3$ = 85˚, N 90˚ E, axial plane (hinge surface) = N 319˚ E/86˚, hinge line = N 319˚ E/4˚, rake (pitch) = 3˚; **4)** *thrust fault*, found in the red marl-chert layer and calcareous shale unit with direction of N 145˚

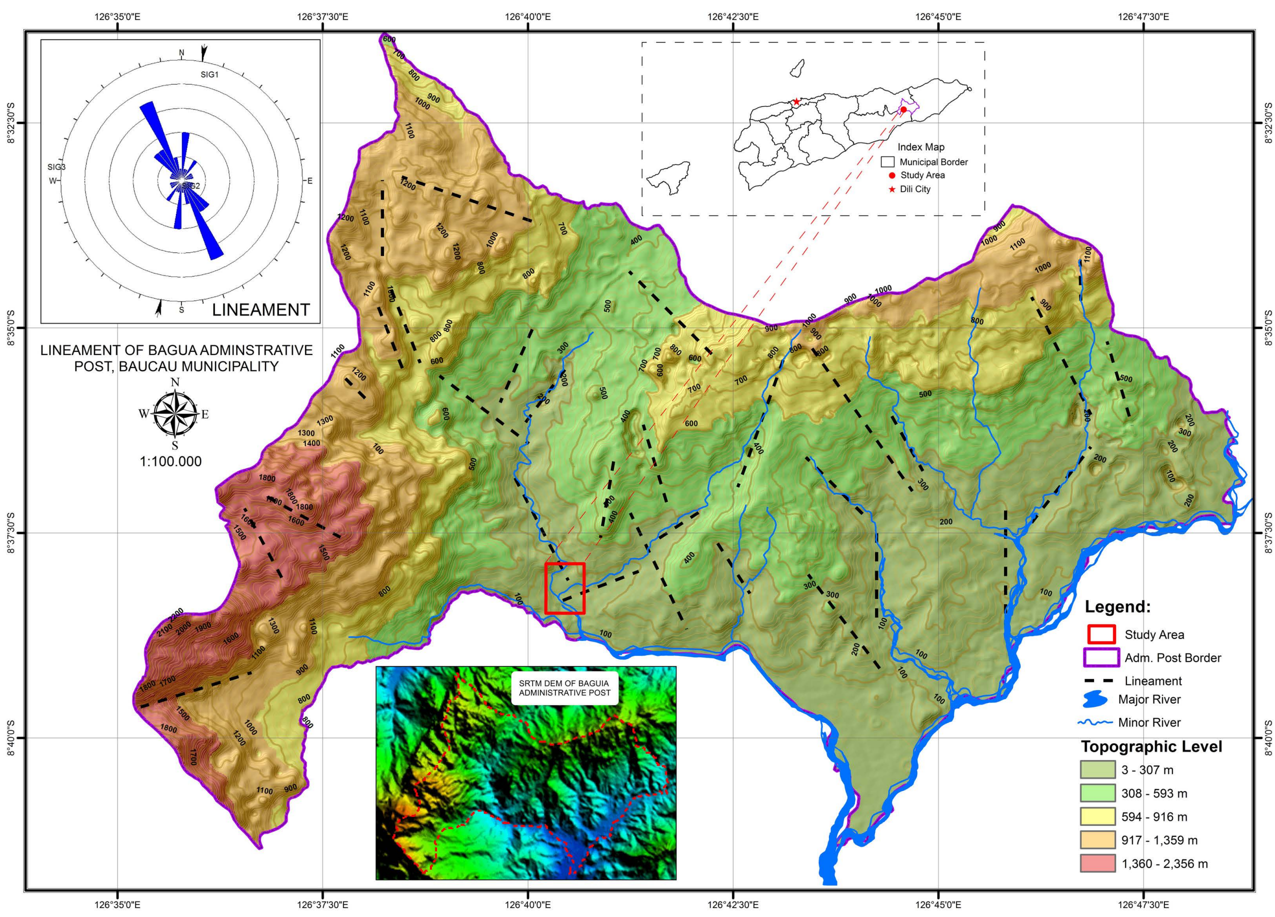

Figure 4. The DEM (*Digital Elevation Model*) lineament interpretation of Baguia administrative post.

E/40˚. The *thrust fault* is crossed by the *left slip fault* from the North to South direction (Figure 5).

Resistivity Interpretation

Using the geological reconnaissance map of the Lacamutu River area of Alaua Kraik, four (4) resistivity lines were selected to interpret the subsurface lithology to 130 m depth (Figure 5 and Figure 6). All these resistivity points are interpreted based on the numbers in Figure 2, Table 5, and the geological reconnaissance map of the study area. The geological cross-section lines of the study area depict the three (3) types of rock units and the documented structural features (Figure 5).

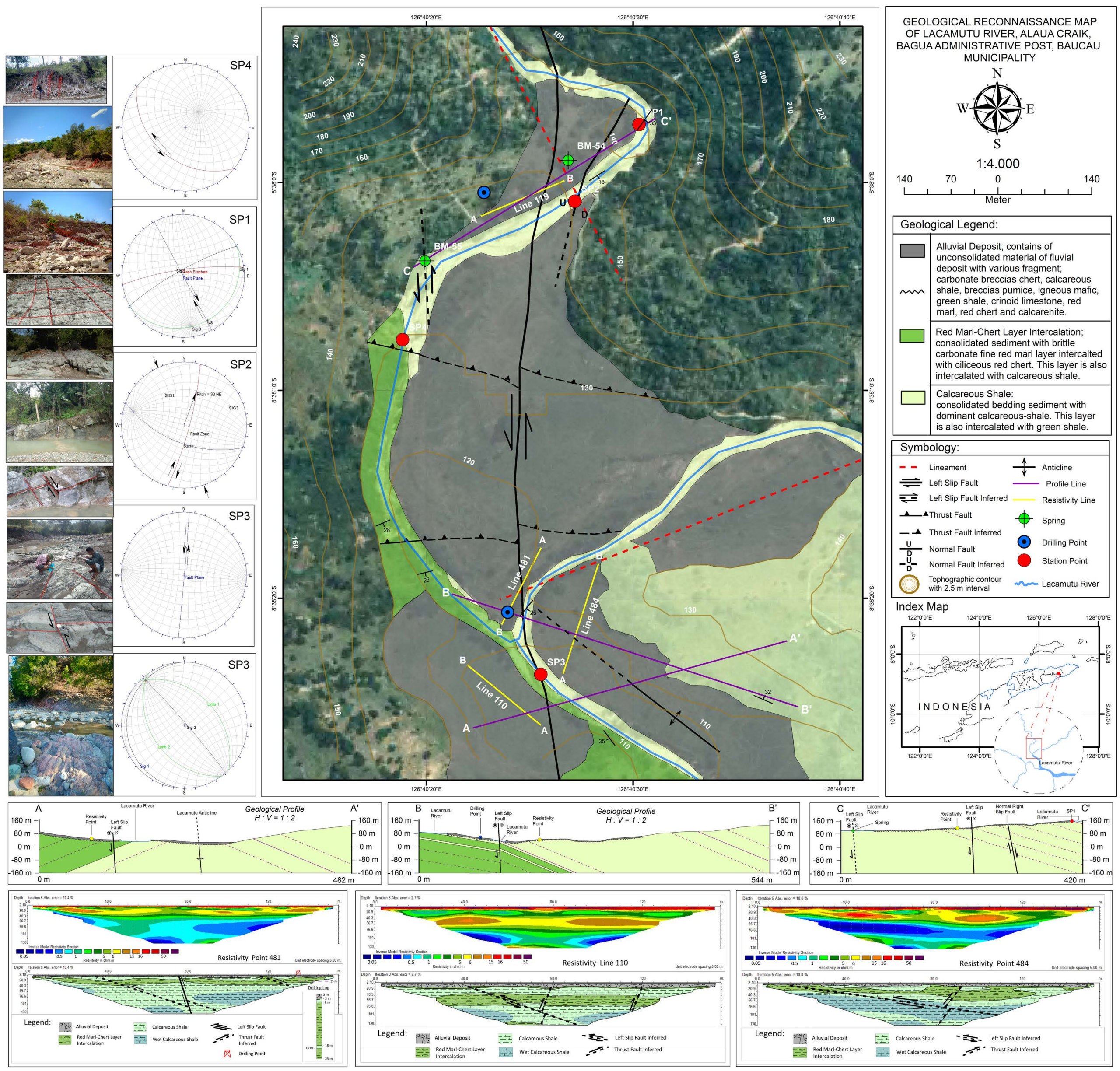

Figure 5. The geological reconnaissance map with profile line of selected resistivity points in Lacamutu River area of Alaua Kraik, Baguia Administrative Post, Baucau Municipality, Timor-Leste.

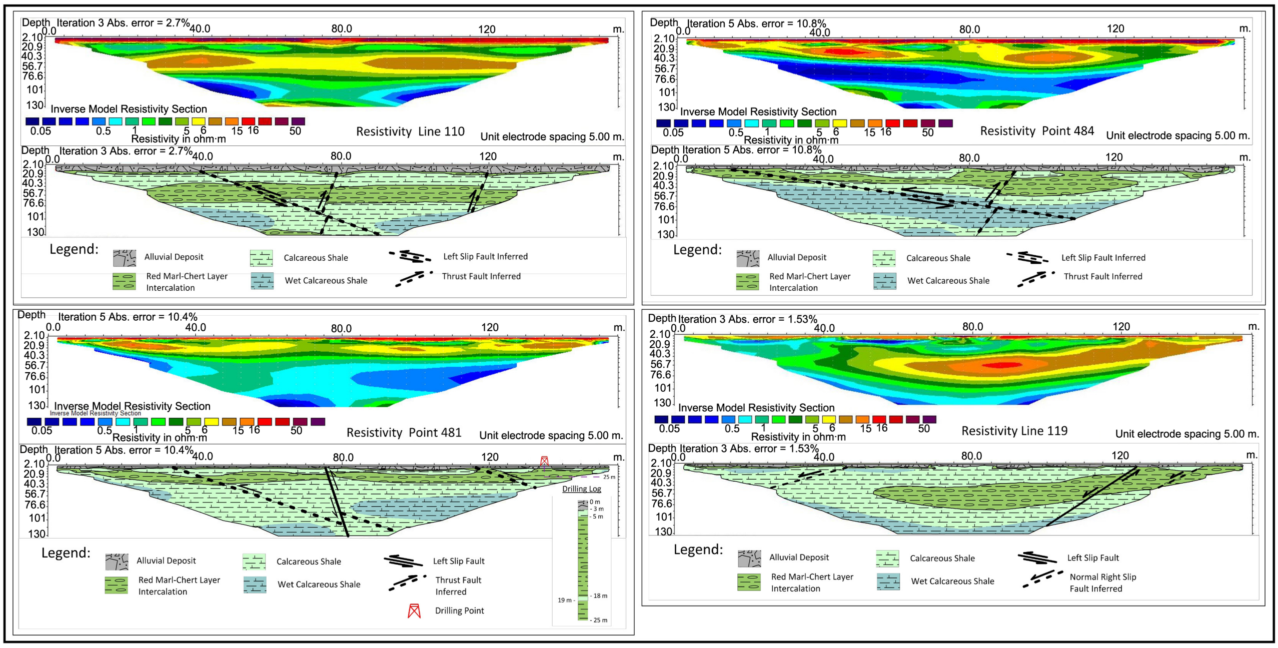

Figure 6. The interpretation of resistivity lines based on the geological reconnaissance map of Lacamutu River Alaua Kraik area, Baguia Administrative Post, Baucau Municipality.

The interpretation of resistivity lines demonstrates that the three (3) rock units are present in the subsurface. The alluvial deposit has a resistivity value ranging from 16 - 50 Ω·m; the intercalated red marl-chert has resistivities ranging from 6 - 15 Ω·m; and the calcareous shale resistivity ranges from 1 - 5 Ω·m and wet calcareous shale from 0.05 - 0.5 Ω·m. These impermeable materials are fractured, with these fractures conduits for surface water resulting in the wet calcareous shale (Figure 6).

Groundwater Potential of the Study Area

To define the groundwater potential in the study area, it is necessary to know the aquifer system, its hydrostratigraphic units, groundwater flow direction, and rainfall. The key to this is understanding the porosity and permeability of the rock units defined previously. All three rock units documented have good porosity but low permeability and represent poor aquifers (Table 2 and Table 3). Whilst the fluvial rock unit is permeable the thinness of the unit and the low permeabilities, driven by the mud matrix, render it a poor aquifer that cannot store nor pass significant volume of water. This also applies to the impermeable calcareous shale unit and the impermeable red marl-chert unit. Because of this, the Lacamutu River has a small discharge and is often dry especially in the dry season.

Aquifer system, hydrostratigraphic units, and groundwater flow conceptualization

The character and distribution of aquifer systems are controlled by lithological, stratigraphical, and structural factors. Due to these geological factors the rock units in the study area have different hydrogeological features. This is largely due to deformation generating fractures and turning lithologic confining units into localized aquifers and permeable-impermeable characters of unconsolidated rock units into intergranular alluvial aquifer. The geological reconnaissance map, resistivity study and well-log data in the study area show that the unconsolidated permeable material of alluvial deposit represents an *intergranular low productivity aquifer system* hydrostratigraphic unit with a thickness of about 3 m. The consolidated impermeable material of red marl-chert layer intercalated with calcareous shale represents a *localized* (*confining unit – fractured*) *low productivity aquifer system* hydrostratigraphic unit with a thickness of more than tens meters. As such, none of these rock units have limited potential to accumulate and pass significant volumes of groundwater [39] (**Figure 7**).

Fractures may both increase or decrease porosity and permeability. Fractured rocks will have good permeability when fractures are open, interconnected, not cemented and can provide conduits groundwater flow [40]. Groundwater flows in an aquifer generally bounded by hydrogeological boundaries such as rocks, faults, folds, or surface water bodies where the main flow directions in the

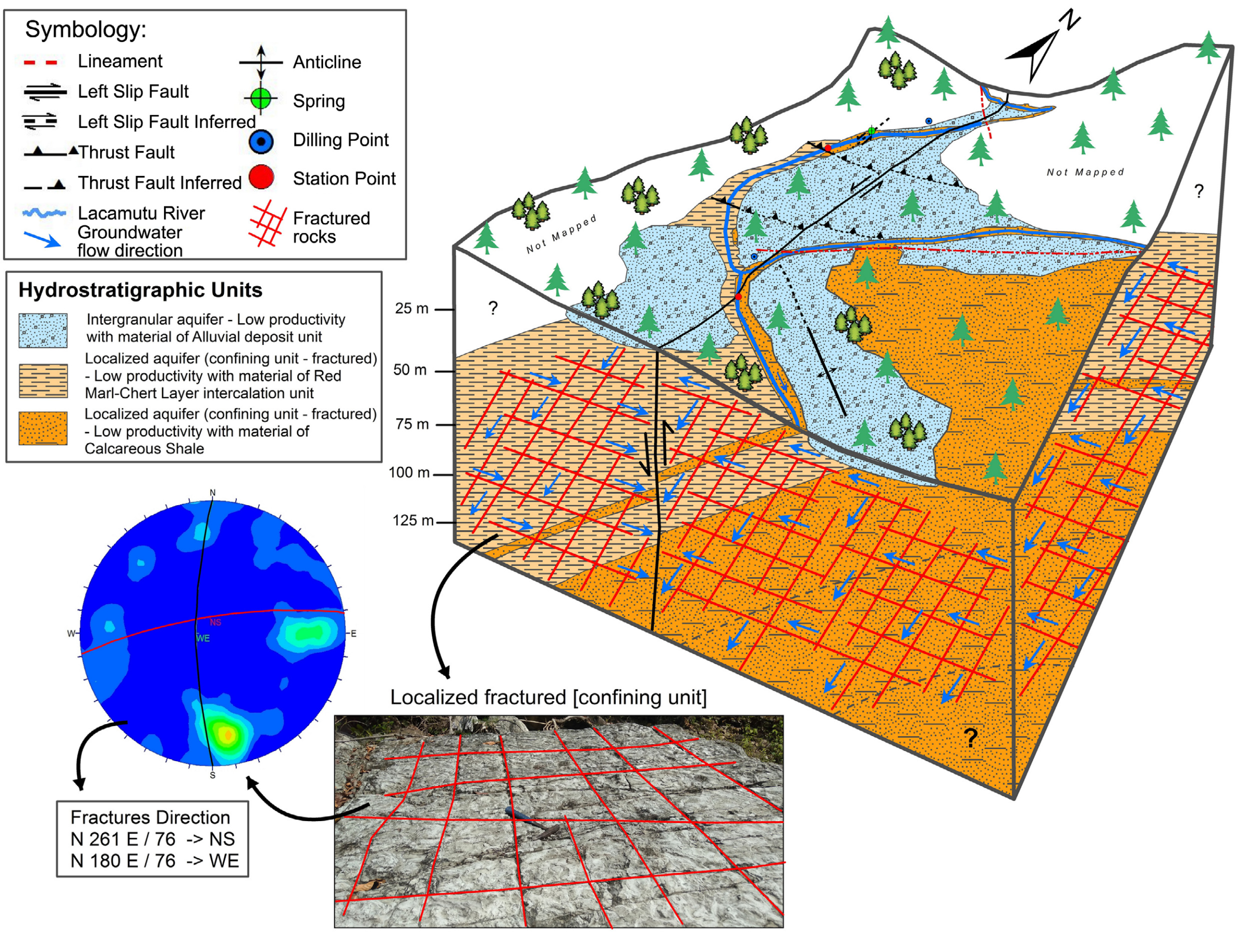

Figure 7. The aquifer system, the hydrostratigraphic units, and the groundwater flow direction modeling concept of the study area.

fractures rocks of confining units are along the joint zone, fault zone, and discontinuity plane zone [24]. In the study area, the groundwater flow naturally controlled by the structural features with flow via the existing fractures of joint largely towards the left slip fault plane zone in the North to South direction. The groundwater on the west side flows through lateral fractures while the groundwater on the east side flows thru vertical fractures all from shear joints to the left slip fault where the controlling factors are pressure, temperature, coarseness, gravity, and geometry (**Figure 7**). The rock units in the study area generally have good intergranular porosity (**Table 2**) and interconnected fractures (**Figure 7**), however they have lower permeability values (**Table 3**) and represent poor aquifers (**Table 4**) due to the increased temperature by depth, compactness, cementation, age, weathering level, and rocks types.

Rainfall

One of the factors to characterise the groundwater potential in the study area are rainfall intensity, maximum rate of runoff, and infiltration. The average monthly rainfall in the study area from 2010 to 2018 is 210.70 mm with the median daily rainfall intensity being 23.64 mm/hour (**Figure 8**). Referring to the classification of rainfall from [41], the monthly rainfall and daily rainfall intensity in the study area are classified as moderate rainfall. With a rain catchment area of 0.95 km^2, a runoff coefficient of 0.7 for *sandy soil lawn – 2% slope* [36] and an average daily rainfall intensity of 23.64 mm/hour, the maximum rate of runoff (Q) for the study area is 0.044 m^3/s or 158.4 m^3/hour. With an infiltration capacity (k) 40% for alluvial deposit and red marl-chert intercalated with calcareous shale (**Table 1**) and 158.4 m^3/hour maximum rate of runoff (Q), the infiltration which occurred in the study area is 63.36 mm/s or 228,096 mm/hour.

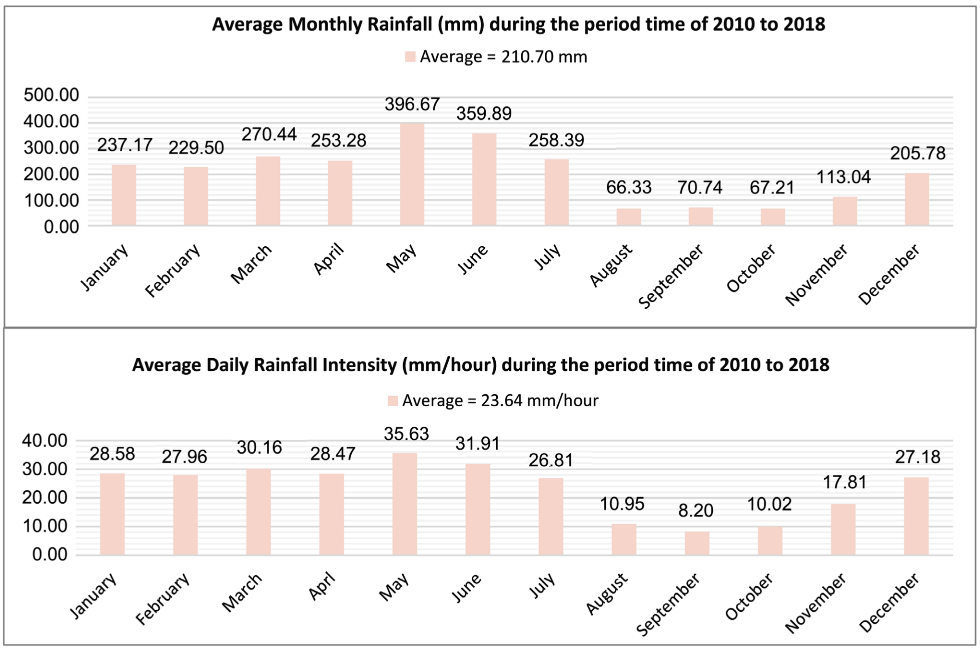

Figure 8. The graph of average monthly rainfall (top) and daily rainfall intensity (bottom) in the study area during the period time of 2010 to 2018 [34].

According to the [41], rain with 100 mm precipitation in a catchment area of 1 km^2 is equal to 100,000 m^3 of water. It means that with a median monthly rainfall of 210.70 mm and a catchment area of 0.95 km^2 there will be 200,165 m^3 of rain water, 158.4 m^3/hour surface runoff and infiltration of 228,096 mm/hour or 228.096 m^3/hour. We suspect much of the rainfall in the study area from 2010 to 2018 did not run-off and infiltrate into the ground but was lost to interception, evaporation, and transpiration.

5. Conclusion and Recommendations

Household data for the study area indicate that 35.05% of households are not able to access clean water. This suggests there are no groundwater resources available to the local community. Geological reconnaissance mapping, hydrogeological study, resistivity survey, and well-log interpretation have identified two main rock units in the study area. These are the unconsolidated permeable alluvial deposit unit and the highly fractured consolidated impermeable red marl chert layer interbedded with the calcareous shale unit. These units have good porosity but low permeability and represent poor aquifers. The key geological structures in the study area are *Lacamutu anticline*, *a thrust fault* that is crossed by the *left slip fault* which then forms a *normal right slip fault.* These materials aquifers are categorized as a hydrostratigraphic unit of *intergranular aquifer system with low productivity* and thickness of about 3 m and a *localized aquifer system* (*confining unit—fractured*) *with low productivity* and thickness of more than tens meters. As a result, these hydrostratigraphic units do not have sufficient aquifers to store and pass significant volumes of groundwater, even though the rainfall in the study area is categorized as moderate rainfall; also, the springs and Lacamutu River have low discharge and mostly dry in the dry season. To overcome this condition, it is highly recommended to install a series of canals for clean water supply to the local communities from Mosa-Ira Spring around 8 km from the study area. This spring has a 12 L/sec discharge which meets WHO (*World Health Organization*) water quality standards [12]. Relevant government stakeholders such as BEE.TL (Water and Sanitation Public Enterprise) and PNDS (National Program of Village Development) should also undertake a hydrogeological evaluation of sites before drilling for water to enhance clean water supply to the communities.

Acknowledgements

Expressing our utmost gratitude to the IPG-TL technical staff who were directly involved in this study, starting from the field activities, data acquisition, data processing, data analyzing and data interpretation as well as the laboratory's petrographic analysis as follows; Geophysics & Regional Petroleum Study Team from Task Force with UNTL's internship students and Laboratory & Lithoteca Team from Division of Geological Investigation. Also, our deepest thankfulness to UNTL (National University of Timor-Leste) for providing us with the *Resis-*

tivity Meter McOHM Profiler 4 Instrument and Dr. Eujay McCartain as a proofreader of this paper. We thank the management board at IPG for facilitating the field and laboratory costs, the local people for the collaboration during the study, and the review and editorial board for the efforts.

Conflicts of Interest

The authors declare no conflicts of interest regarding the publication of this paper.

References

[1] Preeja, K.R., Joseph, S., Thomas, J. and Vijith, H. (2011) Identification of Groundwater Potential Zones of a Tropical River Basin (Kerala, India) Using Remote Sensing and GIS Techniques. *Journal of Indian Society Remote Sensing*, **39**, 83-94. https://doi.org/10.1007/s12524-011-0075-5

[2] Hussein, A.Z., Govindu, V. and Nigusse, A.G.M. (2016) Evaluation of Groundwater Potential Using Geospatial Techniques. *Applied Water Science*, **7**, 2447-2461. https://doi.org/10.1007/s13201-016-0433-0

[3] Todd, D.K. and Mays, L.W. (2005) Groundwater Hydrology. 3rd Edition, Wiley, New York, 636.

[4] Okello, C., Tomasello, B., Greggio, N., Wambiji, N. and Antonellini, M. (2015) Impact of Population Growth and Climate Change on the Freshwater Resources of Lamu Island, Kenya. *Water*, **7**, 1264-1290. https://doi.org/10.3390/w7031264

[5] Celik, R. (2019) Evaluation of Groundwater Potential by GIS-Based Multicriteria Decision Making as a Spatial Prediction Tool: Case Study in the Tigris River Batman-Hasankeyf Sub-Basin, Turkey. *Water*, **11**, Article No. 2630. https://doi.org/10.3390/w11122630

[6] Fainstein, R., Rosario, J.D.D.C., Guterres, H.C., Reis, R.P. and Costa, L.T. (2020) Coastal and Offshore Provinces of Timor-Leste—Geophysics Exploration and Drilling. *The Leading Edge*, **39**, 543-550. https://doi.org/10.1190/tle39080543.1

[7] Kumar, A., Sharma, M.P. and Yadav, N.S. (2014) Assessment of Water Quality Changes at Two Locations of Chambal River: M.P. *Journal of Materials and Environmental Science*, **5**, 1781-1785.

[8] Rajaveni, S.P., Brindha, K. and Elango, L. (2015) Geological and Geomorphological Controls on Groundwater Occurence in a Hard Rock Region. *Applied Water Science*, **7**, 1377-1389. https://doi.org/10.1007/s13201-015-0327-6

[9] Kumar, A., Sharma, M.P. and Taxak, A.K. (2017) Analysis of Water Environment Changing Trend in Bhagirathi Tributary of Ganges in India. *Desalination and Water Treatment*, **63**, 55-62. https://doi.org/10.5004/dwt.2017.20159

[10] Kumar, A., Taxak, A.K., Mishra, S. and Pandey, R. (2021) Long Term Trend Analysis and Suitability of Water Quality of River Ganga at Himalayan Hills of Uttarakhand, India. *Environmental Technology & Innovation*, **22**, Article ID: 101405. https://doi.org/10.1016/j.eti.2021.101405

[11] Khan, M.Y.A., ElKashouty, M., Subyani, A.M., Tian, F. and Gusti W. (2022) GIS and RS Intelligence in Delineating the Groundwater Potential Zones in Arid Regions; A Case Study of Southern Aseer, Southwestern Saudi Arabia. *Applied Water Science*, **12**, Article No. 3. https://doi.org/10.1007/s13201-021-01535-w

[12] IPG-TL (2022) Groundwater Resources Identification for Water Supply to the Community in Baguia Administrative Post, Baucau Municipality, Instituto do

Petróleo e Geologia—Instituto Publico (IPG-IP) Division of Hydrogeology & Mineral Resources, Hydrogeology Team, Rua Delta I, Aimutin, Comoro, Dili, Timor-Leste, Unpublished Report.

[13] Hamilton, W. (1979) Tectonics of the Indonesian Region. USGS Numbered Series No. 1078, U.S. Government Publishing Office, Washington DC, 1-335. https://doi.org/10.3133/pp1078

[14] Harris, R.A. (2006) Rise and Fall of the Eastern Great Indonesian Arc Recorded by the Assembly, Dispersion and Accretion of the Banda Terrane, Timor. *Gondwana Research*, **10**, 207-231. https://doi.org/10.1016/j.gr.2006.05.010

[15] Audley-Charles, M.G. (2011) Tectonic Post-Collision Processes in Timor. *Geological Society*, *London*, *Special Publications*, **355**, 241-266. https://doi.org/10.1144/SP355.12

[16] Hall, R. and Sevastjanova, I. (2012) Australian Crust in Indonesian. *Australian Journal of Earth Sciences*, **59**, 827-844. https://doi.org/10.1080/08120099.2012.692335

[17] Sevastjanova, I., Hall, R., Rittner, M., Paw, S.M.T.L., Naing, T.T., Alderton, D.H. and Comfort, G. (2016) Myanmar and Asia United, Australia Left Behind Long Ago. *Gondwana Research*, **32**, 24-40. https://doi.org/10.1016/j.gr.2015.02.001

[18] Haig, D.W., Rigaud, S., McCartain, E., Martini, R., Barros, I.S., Brisbout, L., Soares, J., Nano, J. (2021) Upper Triassic Carbonate-Platform Facies, Timor-Leste: Foraminiferal Indices and Regional Tectonostratigraphic Association. *Palaeogeography*, *Palaeoclimatology*, *Palaeoecology*, **570**, Article ID: 110362. https://doi.org/10.1016/j.palaeo.2021.110362

[19] Audley-Charles, M.G. (1968) The Geology of Portuguese Timor. *Geological Society*, *London*, *Memoirs*, **4**, 4-84. https://doi.org/10.1144/GSL.MEM.1968.004.01.02

[20] Partoyo, E., Hermanto, B. and Bachri, S. (1995) Geological Map of Baucau Quadrangle, East Timor. Geological Research and Development Centre, Indonesia.

[21] Todd, D.K. (1980) Groundwater Hydrology. 2nd Edition, John Willey & Sons, New York.

[22] Asdak, C. (2007) Hidrologi dan Pengelolaan Daerah Aliran Sungai, Edisi VI. Gadjah Mada University Press, Daerah Istimewa Yogyakarta.

[23] Irawan, D.E. and Puradimaja, D.J. (2015) Hidrogeologi Umum, Perpustakaan Nasional: Katalog Dalam Terbitan, Penerbit Ombak, Yogyakarta.

[24] Prastistho, B., Pratiknyo, P., Rodhi, A., Prasetyadi, C., Ridwan Massora, M. and Kurnia Munandar, Y. (2018) Hubungan Struktur Geologi dan Sistem Airtanah, Kementrian Riset, Teknologi dan Pendidikan Tinggi, Universitas Pembangunan Nasional "Veteran" Yogyakarta, Lembaga Penelitian dan Pengabdian Kepada Masyarakat.

[25] Freeze, R.A. and Cherry, J.A. (1979) Groundwater. Prentice-Hall Inc., Englewood Cliffs.

[26] Earle, S. and Panchuk, K. (2019) Physical Geology: Chapter 14. Groundwater. 2nd Edition, BCcampus, Victoria, 454-pp.

[27] Suharyadi (1984) Geohidrologi (Ilmu Air Tanah) Fakultas Teknik, Universitas Gadja Mada, Yogyakarta.

[28] Fajana, A.O. (2020) Groundwater Aquifer Potential Using Electrical Resistivity Method and Porosity Calculation: A Case Study. *NRIAG Journal of Astronomy and Geophysics*, **9**, 168-175. https://doi.org/10.1080/20909977.2020.1728955

[29] Loke, M.H. (2004) Tutorial: 2-D and 3-D Electrical Imaging Surveys. Geotomo-

Software.

[30] Palacky, G.J. (1988) 3. Resistivity Characteristics of Geologic Targets. In: Nabighian, M.N., Ed., *Electromagnetic Methods in Applied Geophysics*: *Theory*, Vol. 1, Society of Exploration Geophysicists, Houston, 53-129. https://doi.org/10.1190/1.9781560802631.ch3

[31] Telford, W.M. (1976) Applied Geophysics. Cambridge University Press, Cambridge.

[32] Suyono, S. (1978) Hidrologi Untuk Pengairan, PT. Pradnya Paramita, Jakarta.

[33] Telford, W.M. Geldart, L.P., Sheriff, R.E. and Keys, D.A. (1990) Applied Geophysics. 2nd Edition, Cambridge University Press, Cambridge, 770 p.

[34] DNGRA [Diresaun Nasional do Gestaun da Recurso da Agua] (2019) Annual Report of Daily Data: Total Daily Rainfall from the year 2010-2018, Rainfall Station of Baguia Administrative Post - Municipality Baucau, Diresaun Nasional do Gestaun da Recurso da Agua (DNGRA).

[35] Hudson, N.W. (1993) Field Measurement of Soil Erosion and Runoff. Food and Agriculture Organization of the United Nations, Rome.

[36] Hill, J. (2002) Evaluation of Rational Method "C", Update for Manual Revision.

[37] Rickard, M. (1972) Fault Classification: Discussion. *GSA Bulletin*, **83**, 2545-2546. https://doi.org/10.1130/0016-7606(1972)83[2545:FCD]2.0.CO;2

[38] Fluety, M.J. (1964) The Description of Folds. *Proceedings of the Geologist' Association*, **75**, 461-492. https://doi.org/10.1016/S0016-7878(64)80023-7

[39] Wallace, L., Sundaram, B., Brodie, R.S., Marshall, S., Dawson, S., Jaycock, J., Stewart, G. and Furness, L. (2012) Vulnerability Assessment of Climate Change Impacts on Groundwater Resources in Timor-Leste: Summary Report. Geoscience Australia, Canberra. https://doi.org/10.11636/Record.2012.055

[40] Singhal, B.B.S. and Gupta, R.P. (2010) Applied Hydrogeology of Fractured Rocks. 2nd Edition, Springer, Dordrecht, Heidelberg, London. https://doi.org/10.1007/978-90-481-8799-7

[41] BMKG [Badan Meteorologi, Klimatologi, dan Geofisika] (2008) Curah Hujan dan Potensi Gerakan Tanah. Badan Meteorologi, Klimatologi dan Geofisika, Indonesia.